Mon. Not. R. Astron. Soc. **000**, 000–000 (1996)

Optical Polarisation and X-ray data on the AM Her star RE J1844–74

Gavin Ramsay[1,2], Mark Cropper[2], Kinwah Wu[3] & Stephen Potter[2]
[1] *Astronomical Institute, University of Utrecht, Postbus 80000, 3508 TA Utrecht, The Netherlands*
[2] *Mullard Space Science Laboratory, University College London, Holmbury St.Mary, Dorking, Surrey, RH5 6NT*
[3] *Research Center for Theoretical Astrophysics, School of Physics, The University of Sydney, NSW 2006, Australia*

Accepted: April 1996

ABSTRACT

We report optical and X-ray observations made of the AM Her system RE J1844–74 using the AAT and *ROSAT*. From previously published and these new data we have derived a new accurate ephemeris for the spin period of the white dwarf. We find we cannot simultaneously fit the green and red polarisation data. However, we can fit them separately using different values of the plasma parameter, Λ. We investigate the possible reasons for this result. Furthermore, we find that the polarisation data require long narrow accretion arcs. This is in contrast with results on eclipsing AM Her systems which tend to favour accretion regions which are relatively small. We briefly explore the possible effects which may influence the determination of size of the accretion region from these different methods. We have found evidence for the main accretion region of RE J1844–74 to have a magnetic field strength ~10MG less than its secondary pole and the system inclination is moderately high. Our X-ray data are out of phase with the optical data and conclude that this is consistent with our current view of the accretion flow in AM Her systems.

Key words: accretion -binaries: close - Stars: AM Her stars - stars: individual: RE J1844–74 - stars: magnetic fields - cataclysmic variables

1 INTRODUCTION

During the course of the *ROSAT* all-sky survey many new objects were discovered. In particular ~25 new AM Her stars were found (Beuermann & Burwitz 1995): close binary stars in which matter transfers via Roche lobe overflow from a dwarf secondary star onto a magnetic white dwarf primary. The magnetic field strength of the white dwarf (B ~10–70MG) is strong enough to synchronise the spin period of the white dwarf with the binary orbital period. The accretion flow attaches on to the field lines of the white dwarf, is directed out of the orbital plane, travels along the magnetic field lines and forms a shock at some height above the white dwarf. The temperature in the post shock region is $\sim 10^8$ K: hot enough for hard X-rays to be emitted. In addition, polarised cyclotron emission is generated by electrons spiraling around the magnetic field lines (see Cropper 1990 for a full review).

One of the new objects discovered during the *ROSAT* all-sky survey was RE J1844–74. Follow up optical observations showed substantial variations in the cycle-to-cycle light curve and showed a high EUV-Optical ratio (O'Donoghue et al. 1993). On the basis of optical photometry and spectroscopy, O'Donoghue et al. suspected that RE J1844–74 was an AM Her system with a period of 90 mins. Bailey et al. (1995) obtained circular polarisation data which showed a peak to peak variation of ~40%, confirming the AM Her identification. Furthermore, they found evidence for two linearly extended accretion regions. To examine this object in more detail, we obtained linear and circular polarisation data and discuss the X-ray data obtained for this object.

2 THE OPTICAL OBSERVATIONS

Optical observations were obtained on 1994 July 1–4 using the Anglo-Australian 3.9m telescope. The Faint Object Polarimeter (FOP) was used with a Tektronix CCD (operating at a temperature of 200K) as the detector. The FOP is a modification of the Taurus II instrument (Unger et al. 1990) in which the Fabry Perot etalon is replaced by a Wollaston prism to produce two images of an object on the detector. In conjunction with a quarter-wave plate this enables the circular polarisation of the star to be determined (see Cropper et al. 1990 for more details of the instrument and the data reduction procedure).

To minimise the contribution of CCD readout noise we used an on-chip bining of 2 by 2 pixels. This gave a binned pixel image scale of 0.84": comparable with the best seeing disc FWHM experienced during the observing run. The integration time was 25 sec with a further 9 sec dead time giving a time resolution of 34 sec. On the nights of 1994 July 1 and 3, an OG570 filter (passband $\sim 5500 - 9500$Å) was used, whilst on the nights of 1994 July 2 and 4, a BG39 filter (passband $\sim 3500 - 6500$Å) was used. In the first half of the night, linear polarisation measurements were obtained (when there was no moon present), whilst in the second half circular polarisation measurements were obtained (when the moon had risen). Observations of polarised and non-polarised standard stars were observed on each night to remove instrumental polarisation. To remove contamination caused by non-photometric conditions which were present for a small proportion of the time on the nights of July 1 and 2, the intensity light curve was normalised by dividing it by the light curve of a comparison star.

3 THE MEAN OPTICAL LIGHT CURVE

Figure's 1 and 2 show the phase averaged BG39 (green) and OG570 (red) filter data folded such that phase 0.0 is defined as the onset of the bright phase. It can be seen that the orbital cycle can be divided into two distinct sections: a 'bright' and a 'faint' phase. The lead up to the bright phase is characterised by a rapid increase in intensity from the faint phase. This time interval is variable, typically taking $\lesssim$150 sec (similar to that seen in UZ For; Bailey & Cropper 1991). The bright phase shows two distinctive peaks: one at $\phi \sim$0.1 the other at $\phi \sim$0.4. The relative intensity of the first peak compared to the second peak is greater in red light than green although the relative flux is variable in red from cycle to cycle. In the faint phase, lasting from $\phi \sim$0.5–1.0, there is a another peak between $\phi \sim$0.6–0.7 which is more prominent in the green filter. Comparing these data with those shown by Bailey et al. (1995) we find that the relative prominence of the secondary peak at $\phi \sim$0.4 to the primary peak at $\phi \sim$0.1 is much greater in these new data.

The peak polarisation pulse (a maximum of $\sim$8% in red light) occurs at the same point in the orbital cycle as the onset of the sharp fall to the faint phase is seen in red light. Between phases $\phi \sim$0.7–1.0 the linear polarisation is consistent with zero. The position angle of the linear polarisation is well defined during the bright phase when it decreases approximately linearly, unlike the faint phase when the position angle is not well defined. Bailey et al. (1995) do not show any linear polarisation data.

While the degree of linear polarisation is relatively low, the circular polarisation light curve shows a large variation over the orbital cycle: the peak-to-peak variation is $\sim$ 30%. Before the onset of the bright phase, the circular polarisation increases in the positive sense before quickly ($\Delta\phi \sim$0.02) becoming negative. In both the red and green filters the circular polarisation increases (in a negative sense) reaching a maximum of $\sim$–20% at $\phi \sim$0.25.

Comparison with the circular polarisation data shown by Bailey et al. (1995) shows that the circular polarisation changes sign $\phi \sim$0.05 before the onset of the rapid increase in brightness at ϕ=0.0 in contrast to these new data when the change over is near simultaneous. During the descent of the bright phase there are low levels of circular polarisation in these new data: in contrast to that of the observations reported by Bailey et al. (1995). These contrasts will be discussed further below.

4 CYCLE-TO-CYCLE VARIATIONS IN THE OPTICAL LIGHT CURVE

To indicate the cycle-to-cycle variation, we plot the red data in figure 2 as a function of orbital period. Looking initially at the intensity variation, we find that the relative strength of the two peaks of the bright phase is variable. For instance in cycle 16972 the peak at $\phi \sim$0.1 is approximately twice the intensity of the peak at $\phi \sim$0.35 (the cycle number is defined as the number of cycles after the initial epoch of the ephemeris derived in §5). This is in contrast to the majority of orbital cycles where the relative intensity is nearly equal.

Moving to the linear polarisation data, we find that there is also a significant variation between orbital cycles. The prominent linear polarisation peak at $\phi \sim$0.5 is seen to be double peaked on at least 2 out of the 5 occasions where the phase interval was adequately covered. However on 2 occasions there was no evidence of a double peak. The variations in the circular polarisation data are less dramatic, although present. Similar cycle to cycle variations are seen in the green filter.

5 THE EPHEMERIS

The light curve of RE J1844–74 is characterised by a sharp rise leading up to the bright phase (similar to that seen on occasions in the eclipsing AM Her star UZ For; Bailey & Cropper 1991, Ramsay et al. 1993). This sharp rise was observed on 19 occasions in our optical data, the timings of which are shown in table 1. In addition, a further 4 timings of the start of the bright phase were obtained using the high speed white light photometry published by O'Donoghue et al. (1993) and kindly supplied in electronic form by O'Donoghue.

A linear fit to the above data yields the following ephemeris:

$$T = HJD2448475.2933(2) + 0.06255330(2)E$$

where the error on the last significant figure is in brackets. This is significantly more accurate than the ephemeris of O'Donoghue et al. (1993) who derived the period from fitting the photometric primary minimum. By phasing the light curves of the data presented here and the data of O'Donoghue, it is unlikely that the above fit is a cycle alias of the true orbital period.

6 THE X-RAY DATA

RE J1844–74 was observed in X-rays (0.1–2.0keV) using the *ROSAT* satellite on 4 occasions in the pointed mode. On the first two occasions it was observed using the PSPC, while on the latter two it was observed using the High Resolution

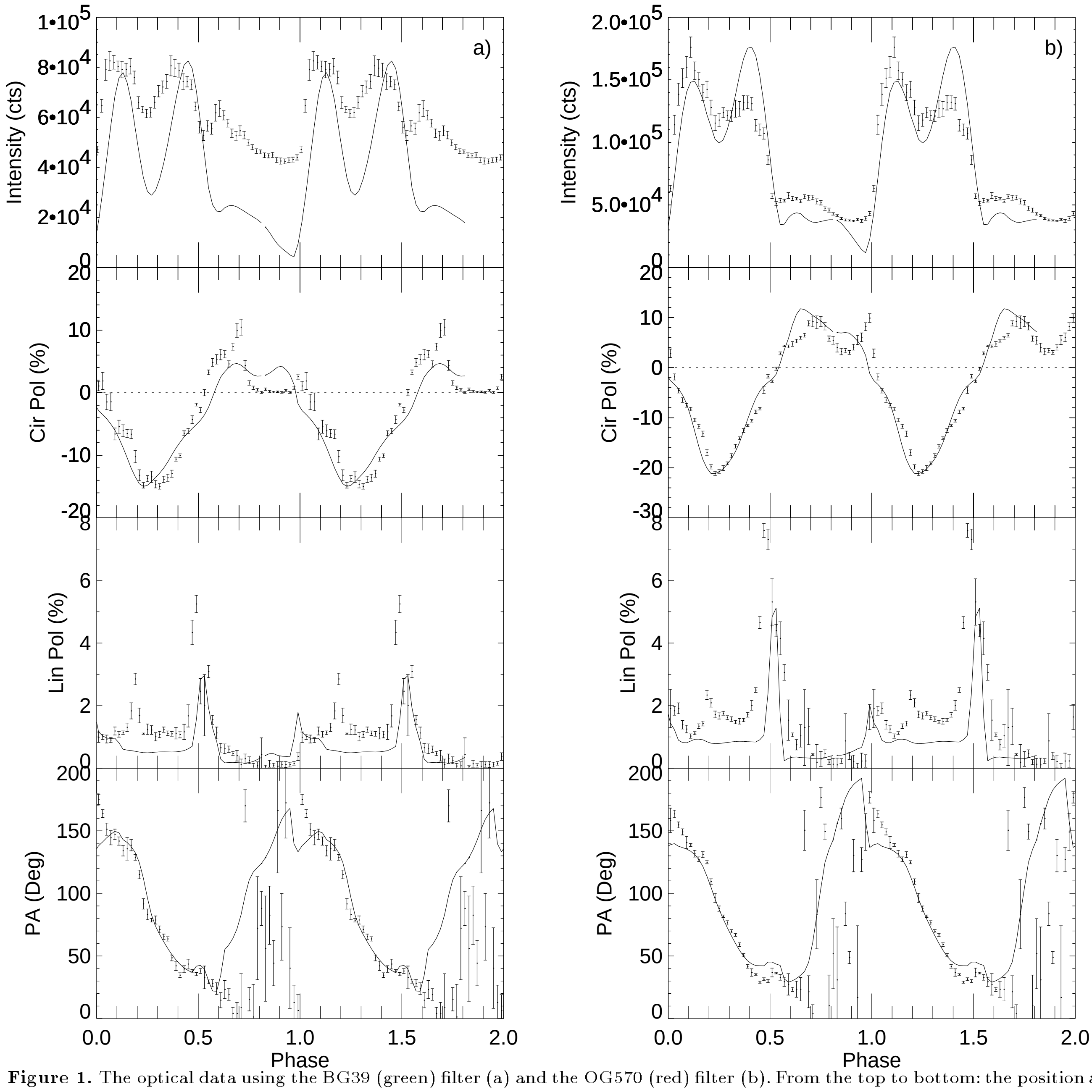

Figure 1. The optical data using the BG39 (green) filter (a) and the OG570 (red) filter (b). From the top to bottom: the position angle of the linear polarisation (deg), the linear polarisation (%), the circular polarisation (%), and the intensity as a function of orbital phase. The best model fits are overlaid (see §7).

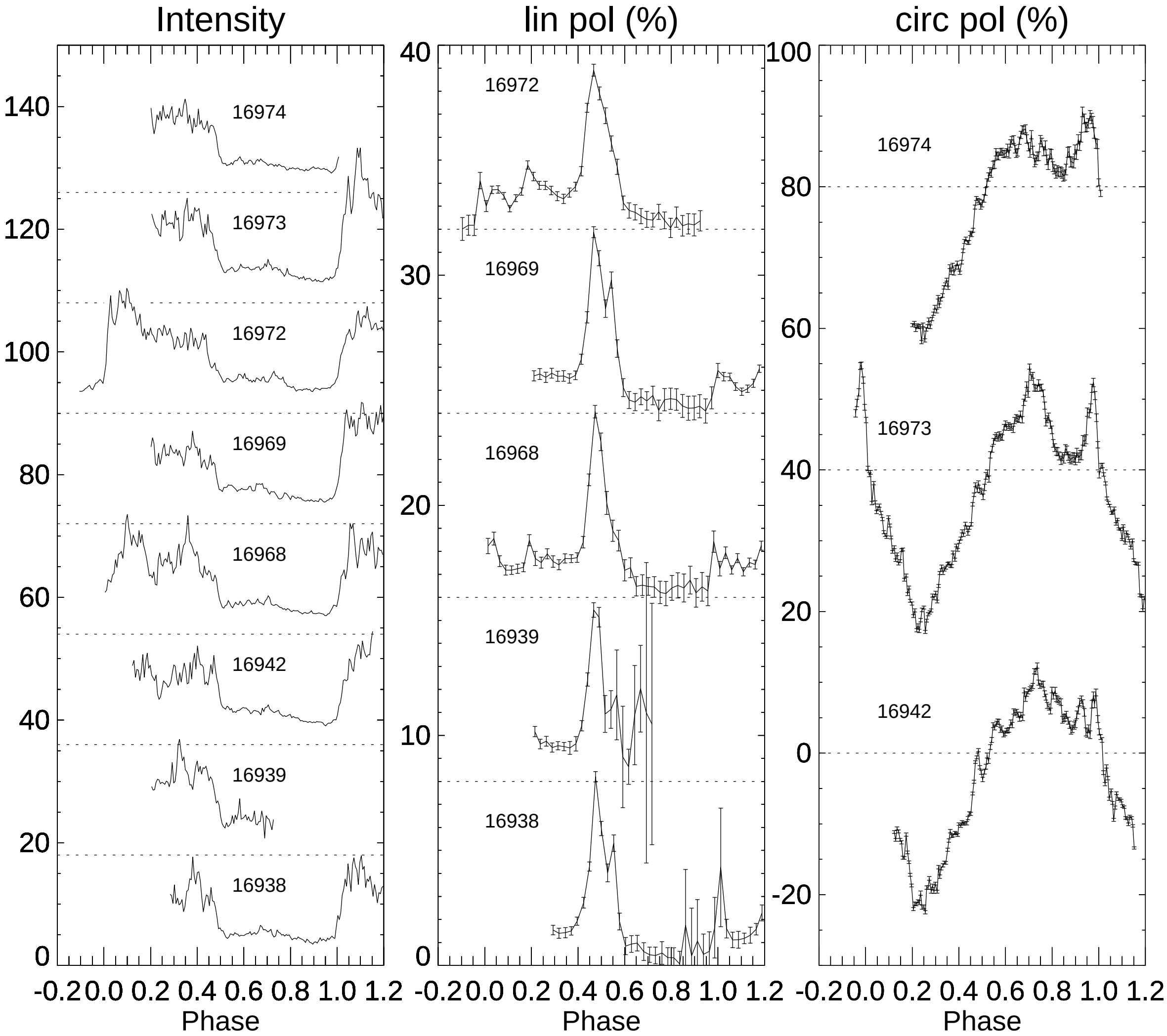

Figure 2. The optical OG570 (red) data as a function of orbital cycle. From left to right: the intensity (arbitrary units), the linear polarisation and the circular polarisation. The number in each panel refers to the number of cycles after the zero epoch of the ephemeris of the orbital period. Each data group is displaced upwards by 20 units in intensity, 8% in linear polarisation and 40% in circular polarisation.

HJD	+/-	HJD	+/-
8475.293900	0.0003	9536.260714	0.0005
8477.294690	0.0003	9536.322496	0.0005
8477.358190	0.0003	9536.947746	0.0005
8478.296450	0.0003	9537.009760	0.0005
8532.279700	0.0005	9537.135303	0.0005
8532.341700	0.0005	9537.197456	0.0005
8533.279000	0.0005	9537.260071	0.0005
8533.343000	0.0005	9537.322871	0.0005
9535.070327	0.0005	9537.886200	0.0005
9535.320881	0.0005	9537.949383	0.0005
9536.010265	0.0005	9538.011662	0.0005
9536.072243	0.0005	9538.199323	0.0005
9536.134083	0.0005	9538.262216	0.0005
9536.197416	0.0005		

Table 1. The timings of the sharp rise from the faint phase (HJD-2440000.0).

Imager (HRI) (see table 2). We used the **EXSAS** data analysis package (Zimmermann et al. 1994) to extract a time series for the object plus background using an aperture centered on the source. In determining the size of the aperture, a compromise was made between sampling as many of the source photons as possible (the point-spread-function for very soft photons, which predominate in objects such as AM Her stars, is relatively large in the PSPC) and optimising the signal-to-background ratio. The source was on-axis in both the PSPC and HRI observations. The background level was determined from a source free region of sky then subtracted from the source with appropriate scaling for the solid angles involved.

The X-ray data were folded on the ephemeris derived above and plotted in figure 3. (The ephemeris is sufficiently accurate that we can be sure of the relative phasing to within 0.01 cycles). The X-ray data taken during 1992 October showed a peak count rate twice that of the data taken during 1993 March. The HRI count rate was similar at both epochs and corresponds roughly to a count rate of $\sim$1cts s^{-1}in the PSPC, implying that it was in a lower accretion state than

Date	Exposure (sec)	Instrument
1992 Oct 18–19	3907	PSPC
1993 Mar 26–30	5681	PSPC
1995 Apr 3–5	9621	HRI
1995 Sept 16–Oct 1	9073	HRI

Table 2. The dates and exposures of the *ROSAT* data used in this study, together with the instrument used.

March 1993. The orbital cycle is unevenly sampled in all 4 X-ray light curves which makes comparison difficult. However it is clear there is substantial cycle-to-cycle and epoch-to-epoch variations in the light curves. Furthermore, in 3 of the 4 epochs the peak in X-rays does not correspond to the peak optical brightness, which consistently lies between $\phi \sim 0.1 - 0.4$. In addition there is evidence that the 'on' X-ray state moves in phase.

Ramsay et al. (1994) presented the spectral parameters for the observation made on 1992 October. They found that the ratio of the soft-to-hard X-ray luminosity in RE J1844-74 was not very well constrained, but was consistent with that expected from the standard shock model of Lamb & Masters (1979). This is in contrast with many AM Her stars which show a much larger soft-to-hard X-ray ratio than expected (Ramsay et al. 1994). We extracted a spectrum from the data obtained on 1993 March using a similar technique to that described above for extracting the light curves. We found that this spectrum showed no significant change compared with that obtained on 1992 October. As the HRI has virtually no spectral response we cannot comment on the spectra of the source in 1995.

7 MODELLING THE POLARISATION

7.1 The Model

The polarised radiation from AM Her systems is believed to be cyclotron emission from the shock-heated material at the white dwarf accretion poles. In early studies, the emission region was assumed to have a simple geometry, e.g. a semi-infinite slab (Chanmugam & Dulk 1981) or a point source (Meggitt & Wickramasinghe 1982). If the four-Stokes-parameter formulation is used, the intensity and the polarisations are given by the Stoke vector **I**, which satisfies the radiative transfer equation:

$$\frac{d}{ds}\mathbf{I} = \mathbf{e} - \mathbf{K}\cdot\mathbf{I},$$

where **e** is the emission coefficient, **K** is the absorption coefficient and s is the path length (see Meggitt & Wickramasinghe 1982). When the temperature T, the magnetic field **B**, the electron density n_e and the characteristic size of the emission region s are specified, we can determine the plasma parameter Λ, (Wickramasinghe & Meggitt 1985):

$$\Lambda \;= 2.0\times 10^5\mathrm{cm}\left(\frac{s}{10^5\mathrm{cm}}\right)\left(\frac{n_e}{10^{16}\mathrm{cm}^{-3}}\right)\left(\frac{|\mathbf{B}|}{30\mathrm{MG}}\right)^{-1}$$

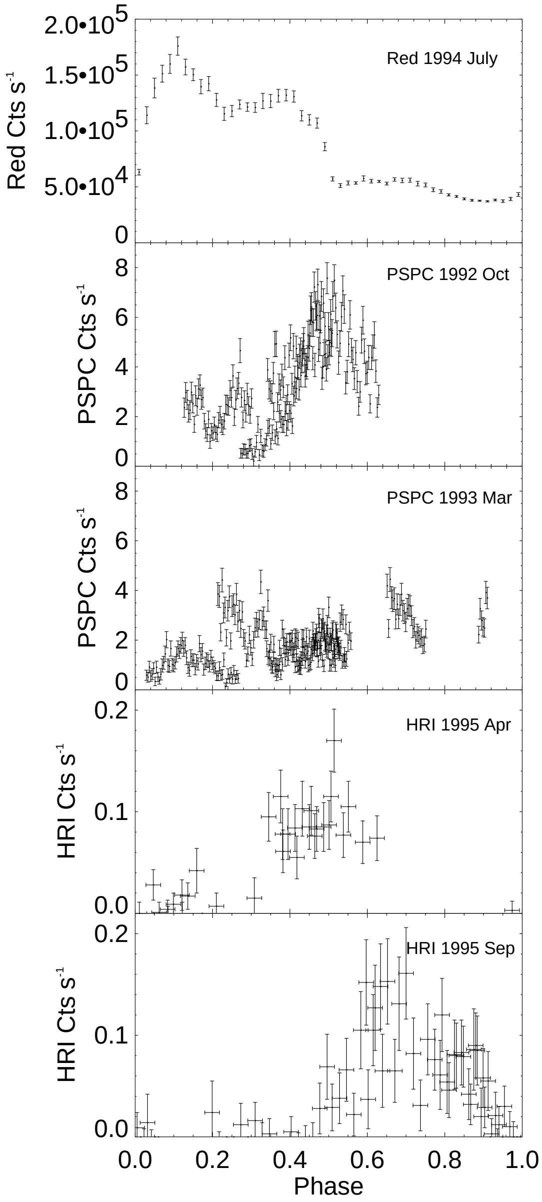

Figure 3. The ROSAT data (0.1–2.0keV) from 4 epochs. The data is folded on the best fit ephemeris where ϕ=0.0 is defined as the sharp rise from the faint phase. For comparison the optical (red) phase folded light curve is shown in the top panel.

We can thus determine the properties of the radiation. Generally, the linear polarisation peaks at the orbital phases where the magnetic field **B** is perpendicular to the line of sight. The circular polarisation is, however, at its minimum at these orbital phases. Conversely, when **B** is approximately parallel to the light of sight, the circular polarisation is at its maximum while the linear polarisation is at its minimum.

Later more detailed observations suggested that the accretion regions are extended and have structures more complex than a point source or a semi-infinite slab (eg Beuermann, Stella & Patterson 1987, Cropper 1989, Ferrario, Wickramasinghe & Tuohy 1989). Moreover, the white dwarfs in AM Her systems were found to have magnetic fields which deviated significantly from a simple centered dipole field (Wu & Wickramasinghe 1993). As the emission regions are extended, T, n_e and $\mathbf{B}$ are not necessary constant. In particular, the variations in the orientation of the magnetic field vector in the emission region complicate the process of modelling the polarisation of the radiation. Further complication can be introduced if the field geometry deviates from a simple dipole. For off-centered dipole fields, the two emission regions may not have the same magnetic field strength and not located exactly 180° apart.

Here, we adopt the model emission region in which, (1) the emission regions are extended and have an arc shape, (2) the location of the emission regions may be far from the magnetic poles, and (3) T and n_e are constant in each emission region. The four-Stokes formulation is used in the radiative transfer calculations, with the emission and absorption coefficients calculated following Meggitt & Wickramasinghe (1982). The Stoke vectors are first determined locally at the white dwarf surface and are then summed to obtain the resultant Stoke vectors. From the resultant Stoke vector, the intensity and the linear and circular polarisations as a function of the orbital phase can be obtained. The model we consider is commonly used in determining the parameters of the emission region for other AM Her systems (eg Cropper & Wickramasinghe 1993, Piirola et al. 1994).

7.2 The results

The most prominent features of the light curves can be modelled using a single accretion region. The rapid increase in the intensity at ϕ=0.00 is most likely due to cyclotron beaming when an accretion region has emerged over the limb of the white dwarf. The rapid decline in red light at ϕ=0.5 is thus due to this accretion region rotating over the edge of the visible surface of the white dwarf.

However, a single accretion region is insufficient to model the finer details of the light curves: the linear polarisation increase at $\phi \sim$0.18 and the extra peak at $\phi \sim$0.57, in addition to the hump in green light at $\phi \sim$0.6. One further unusual feature is the positive circular polarisation between $\phi \sim$0.7–1.0 whereas there is no detectable linear polarisation and the intensity light curve is flat.

We started by modelling the data taken through the red filter and considered several accretion regions of different extent on the surface of the white dwarf such that a crude fit to the light curve was obtained. We modified the magnetic field strength, plasma parameter, the inclination, i, and the colatitude of the magnetic axis, δ, until a solution was found which fitted all 3 polarisation curves relatively well (the temperature was taken to be 10keV).

The model curves are shown with the data in figure 1b. The accuracy of fit is remarkably good: all the major features in the light curves are well reproduced. However, some of the more detailed features in the data are not as well reproduced; for instance, the linear polarisation spike at ϕ=0.2, and the turnup in the circular polarisation at ϕ=0.98. In some of these cases, it was possible to obtain better fits to these sections of data by varying the plasma parameter, and or magnetic field strength. However, this made the fit to other sections of data much worse. Such a feature is evidence for inhomogeneity along the length of the accretion arcs.

The location of the accretion regions, their magnetic field strength and plasma parameter, Λ, for our best fit solution are given in table 3. The arcs are long and thin: over 100° in magnetic longitude. The main accretion arc was modelled as a uniformly bright arc, while the secondary arc was less bright towards its trailing edge. We found an inclination, $i = 80°$, and magnetic co-latitude, $\delta = 30°$ gave best fits to the accretion region. We will discuss the implications of this high value of i in the next section. We show in figure 4 the location of the accretion regions as seen from directly above the magnetic poles.

Although the location of the accretion regions are similar to that found by Bailey et al. (1995) (the location of the secondary accretion region is shorter by 20° in our best fit), the inclination is significantly different: Bailey et al. find $i = 60°$ and $\delta = 130°$. However, Bailey et al. did not have the benefit of linear as well as circular polarimetry. If we model our data using arcs located as before but with $i = 60°$ and $\delta = 130°$ we find a reasonable fit with the circular polarisation data, but a very poor fit to the position angle of the linear polarisation. (The reason for the large difference in the values obtained for δ between our study and Bailey et al. (1995) is due to defining δ=0 at different poles).

We then made a similar fit to the green filter data, using the same values for i, β, the location of the accretion regions, the magnetic field strength of the poles and the plasma parameters of the accretion region. We found that a good fit to the data was not possible. However by increasing the values chosen for the plasma parameter, we found we could get a good fit with the data, although again the finer details of the light curves were not always well fitted (see figure 1). As before, it was possible to improve the fits to sections of the data by varying the plasma parameter and/or the magnetic field strength. However, the goodness of fit to other sections of data got significantly worse.

From the definition of Λ, we can see that Λ is an estimator of the size of the emission region. One might argue that the emission regions for the red and green radiation have different sizes as in the case of the X-rays where the area emitting hard X-rays is smaller than that emitting soft X-rays. This argument is, however, inappropriate. As radiation in both the red and green filters is cyclotron emission from the same region, the sizes of their emission regions should not be different. It has been shown from studies of eclipsing polars that there is no evidence that the emission regions for optical radiation of different wavelengths have different emission region (eg Bailey & Cropper 1991). The difference in Λ obtained from fitting the green and the red radiation is probably due to optical depth effects caused by the temperature and density inhomogeneity in the emission region. Thus, Λ is not a good size estimator if the emission region is inhomogeneous and has a complicated geometry. Alternatively, the difference may be due to an inadequate consideration of field geometry considered in the fitting. However, such possibilities are not easily distinguished and deserves further investigation.

8 DISCUSSION

In the last section we constructed two models which can describe the main features of our red and green optical data. The accretion regions were very extended and narrow with

Accretion Region	Range in mag long (degrees)	Range in mag lat (degrees)	Width of arc (degrees)	B (MG)	Λ(red) (10^6)	Λ(green) (10^6)
Main	80–200	8–28	2	27	0.6	7
Secondary	220–360	160–125	1	38	0.8	8

Table 3. The best fit solutions to the red (OG570) and green (BG39) filter data. We show the location of the accretion regions in magnetic co-ordinates along with their polar magnetic field strength and plasma parameter for a plasma temperature of kT=10keV.

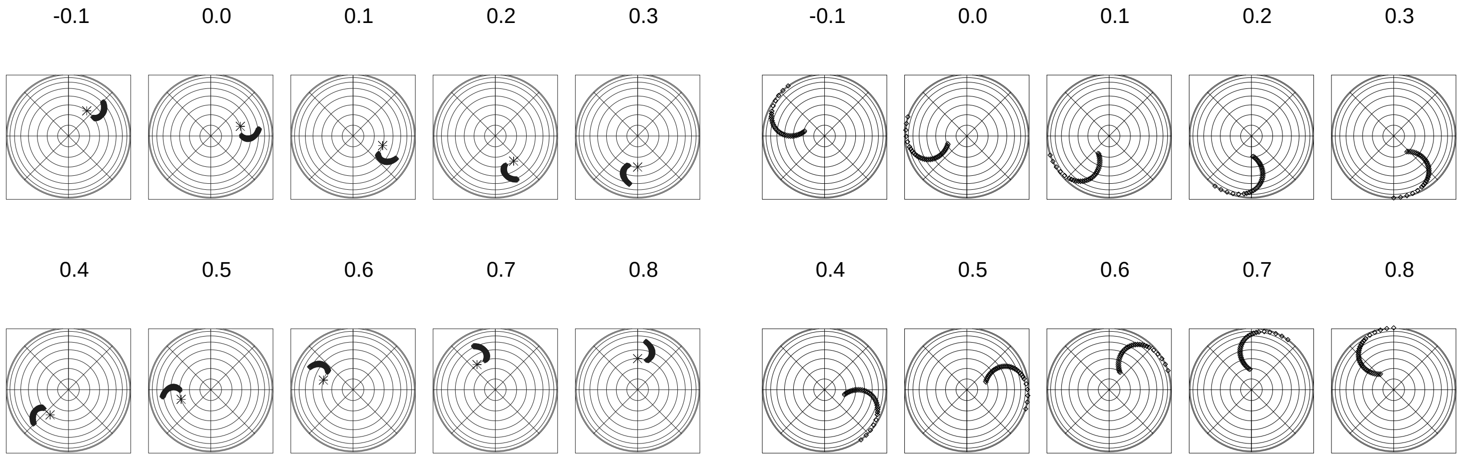

Figure 4. The left hand panel shows the location of the main accretion region when looking directly down on top of the main magnetic pole. Similarly, the right hand panel shows the secondary accretion region when looking directly down on top of the secondary magnetic pole. The magnetic axis is shown by an asterix.

the main region shorter than the secondary, although the secondary was less bright towards the trailing edge. Most importantly, evidence was found for the main pole having a magnetic field strength ~10MG less than the secondary pole. (The field strength that we derive for the main pole is similar to that found by Bailey et al 1995). The result is consistent with that found for other AM Her stars which have been found to show different field strengths at each pole, insofar as the primary pole shows a lower field strength than the secondary pole, suggesting that it is more favourable for accreting material to attach onto field lines from the weaker pole. This is contrary to that predicted from a simple dipole magnetic field but is consistent with that predicted from a dipole-quadrapole magnetic field (Wu et al 1994).

Making an accurate comparison of the optical data with the X-ray data is difficult since the X-ray observations cover only about half the orbital cycle. Furthermore, the optical and X-ray observations were conducted at different epochs. As shown in figures 2 and 3 there are large cycle to cycle variations in the optical and X-ray light curves. This implies that the total as well as the specific accretion rates for the accretion poles may vary significantly from cycle to cycle. However, it is clear that on at least 3 out of 4 epochs when it was observed in X-rays the bulk of the soft X-ray emission originates near the secondary cyclotron emission region. Furthermore, the phase of maximum X-ray emission varies in phase, which may be due to the accretion region varying in longitude over the medium time scale.

The fact that the optical and X-ray peak flux do not coincide is perhaps an indication to the conditions in the accretion stream. The currently accepted view of the accretion flow is one made up of dense 'blobs' of material (which penetrate the photosphere of the white dwarf where they are thermalised and thereby produce the bulk of the soft X-ray emission), and a less dense 'rain' of material which shocks above the surface of the white dwarf (eg Ramsay, Cropper & Mason 1995). It is in this shock region that the cyclotron emission originates. As the accretion stream flows towards the white dwarf, the magnetic field can be thought of as a density filter, in that the less dense rain of material is threaded by the field lines of the magnetic pole pointing towards the secondary star and produces hard X-rays and cyclotron emission. The dense blobs of material can flow further before they are threaded by the pole pointing away from the secondary star and produce soft X-rays. In the case of RE J1844–74, we do not know the location of the secondary star in the binary system. However, our observations are consistent if it is the secondary pole which points away from the secondary star and the bulk of the X-ray emission is in soft X-rays. Although the soft-to-hard X-ray balance is consistent with the hard and soft X-ray fluxes being roughly equal, it is not very well constrained and is equally consistent with the soft X-rays being much more dominant than hard X-rays (Ramsay et al 1994). Such a view is consistent with EUV observations which show it to be EUV bright (O'Donoghue et al. 1993). (The flux in the *ROSAT* WFC survey is comparable to the observed flux in the PSPC, assuming a spectrum similar to that in Ramsay et al 1994).

In our model, we find a best fit solution with an inclination of $i = 80°$. For such a high value for the inclination, the question of RE J1844–74 being an eclipsing system must be addressed. Using the period-secondary mass relation expected for a main-sequence star, $M_2 = 0.11 P_{hr}$ (eg Frank, King & Raine 1992), we find $M_2 \sim 0.16 M_\odot$ for a binary orbital period of 90 mins. Using this result in addition to consideration of the binary separation, we deduce that to avoid eclipses $i \lesssim 73, 78°$ for a white dwarf of mass $0.5, 1.4 M_\odot$ respectively. Although there is some degree of uncertainty associated with determinations of this kind, it is clear that for a system of $i = 80°$, an eclipse is almost certain to take place. There is no convincing evidence for an eclipse in RE J1844-74 in the data we present here. A model fit is dependant on many factors, the physics of the accretion flow being no small matter. Further, although our model fit is good at adequately describing our polarisation data, we cannot be completely certain that it is a unique solution. However, we consider that a high value for the inclination is much more probable than a lower value.

As has been found in many polarisation studies, we have found that we require long thin arcs to get good fits to the optical polarisation data. To give a better understanding of the effect of varying the length of the accretion arcs, we plot in figure 5 the model polarisation curves and the red filter data for the main accretion arc of different length. In this case we have reduced the extent of the trailing edge. The other parameters and the length of the secondary accretion region remain unchanged from that quoted in table 3. From figure 5 we can see that the effect of reducing the main accretion arc by 60° apon the polarisation curves is small: the only noticeable effect is that the goodness of fit of the position angle of the linear polarisation is worse at the ingress and egress of the main accretion region. This effect is accentuated to quite large degrees when the length of the accretion region is reduced even further. It is arguable that the overall fit to the linear polarisation curve is better and that at certain phases a better fit is made with the circular polarisation data. However, the poor fit to the position angle made us favour a long accretion arc rather than a shorter arc. We also varied the length of the secondary arc and found that here, the linear polarisation curve and the position angle variation were not significantly effected by reducing the length of the arc. However, the fit of the model circular polarisation curve was much worse compared with the data for shorter arc lengths. We deduce that the polarisation curves require the presence of long accretion arcs in RE J1844–74. This is in contrast to studies of eclipsing AM Her systems which tend to support the view that the accretion region in AM Her systems is small and roughly circular (eg UZ For: Bailey & Cropper 1991, DP Leo: Bailey et al 1993, Stockman et al 1994, HU Aqr: Glenn et al 1994, and the suspected AM Her system 1H1752+081: Silber et al 1994). One possible factor may be due to the fact that although we can model the red and the green data separately to a good degree, we cannot obtain a model which can simultaneously fit both sets of data. Possible factors contributing to this effect were mentioned previously. A closer analysis of those systems which are eclipsing and have good polarisation data may provide some clues to understanding this problem.

9 CONCLUSIONS

In summary, we have determined a new accurate ephemeris for RE J1844–74 based on the onset of the bright phase. We have modelled the polarisation curves in red and green broad wavebands and found that although a simultaneous fit is not possible, it is possible to fit them separately using different values for the plasma parameter. We find the polarisation curves require accretion regions which are long extended (but narrow) arcs. Furthermore, we have found evidence that the primary accretion pole has a magnetic field strength ~10MG less than the secondary pole and that a high inclination is favoured. We find evidence that the X-ray light curve is variable from cycle-to-cycle and epoch-to-epoch, and that in most epochs the peak of the optical flux and the X-ray flux are in anti-phase. Such a finding is consistent if the bulk of the X-rays are in the form of soft X-rays which the EUV observations suggest is the case.

10 ACKNOWLEDGMENTS

We would like to thank the AAT staff for all their support during our observing run. GR would like to thank the European Union for a fellowship, and SP would like to thank PPARC for a post-graduate studentship. GR would like to thank Dr Peter Wheatley for useful discussions on the accretion flow in AM Hers. We would also like to thank Dr Darragh O'Donoghue for supplying previously published photometry in electronic form. This paper is based partially on data extracted from the *ROSAT* data archive in Garching, Germany.

11 REFERENCES

Bailey, J. A. & Cropper, M., 1991, MNRAS, 253, 27

Bailey, J., Wickramasinghe, D. T., Ferrario, L., Hough, J. & Cropper, M., 1993, MNRAS, 261, L31

Bailey, J. A., Ferrario, L., Wickramasinghe, D. T., Buckley, D. A. H. & Hough, J. H., 1995, MNRAS, 272, 579

Beuermann, K., Stella, L. & Patterson, J., 1987, ApJ, 316, 360

Beuermann, K. & Burwitz, V., 1995, In Proc *Cape Workshop on MCVs*, p.99, ASP Conf Series, Vol. 85

Chanmugam, G. & Dulk, G. A., 1981, ApJ, 244, 569

Cropper, M., 1989, MNRAS, 236, 935

Cropper, M., 1990, Space Sci Rev., 54, 195

Cropper, M. & Wickramasinghe, D. T., 1993, MNRAS, 260, 696

Cropper, M., Bailey, J. A., Wickramasinghe, D. T., Ferrario, L., 1990, MNRAS, 224, 34P

Ferrario, L., Wickramasinghe, D. T. & Tuohy, I. R., 1989, ApJ, 341, 227

Frank, J., King, A. R. & Raine, D. J., 1992, Accretion Power in Astrophysics, Cambridge University Press, Cambridge

Glenn, J., Howell, S. B., Schmidt, G. D., Liebert, J., Grauer, A. D., Wagner, R. M., 1994, ApJ, 424, 967

Lamb, D. Q. & Masters, A. R., 1979, ApJ, 234, L117

Meggitt, S. M. A. & Wickramasinghe, D. T., 1982, MNRAS, 198, 71

O'Donoghue, D., Mason, K. O., Chen, A., Hassall, B. J. M. & Watson, M. G., 1993, MNRAS, 265, 545

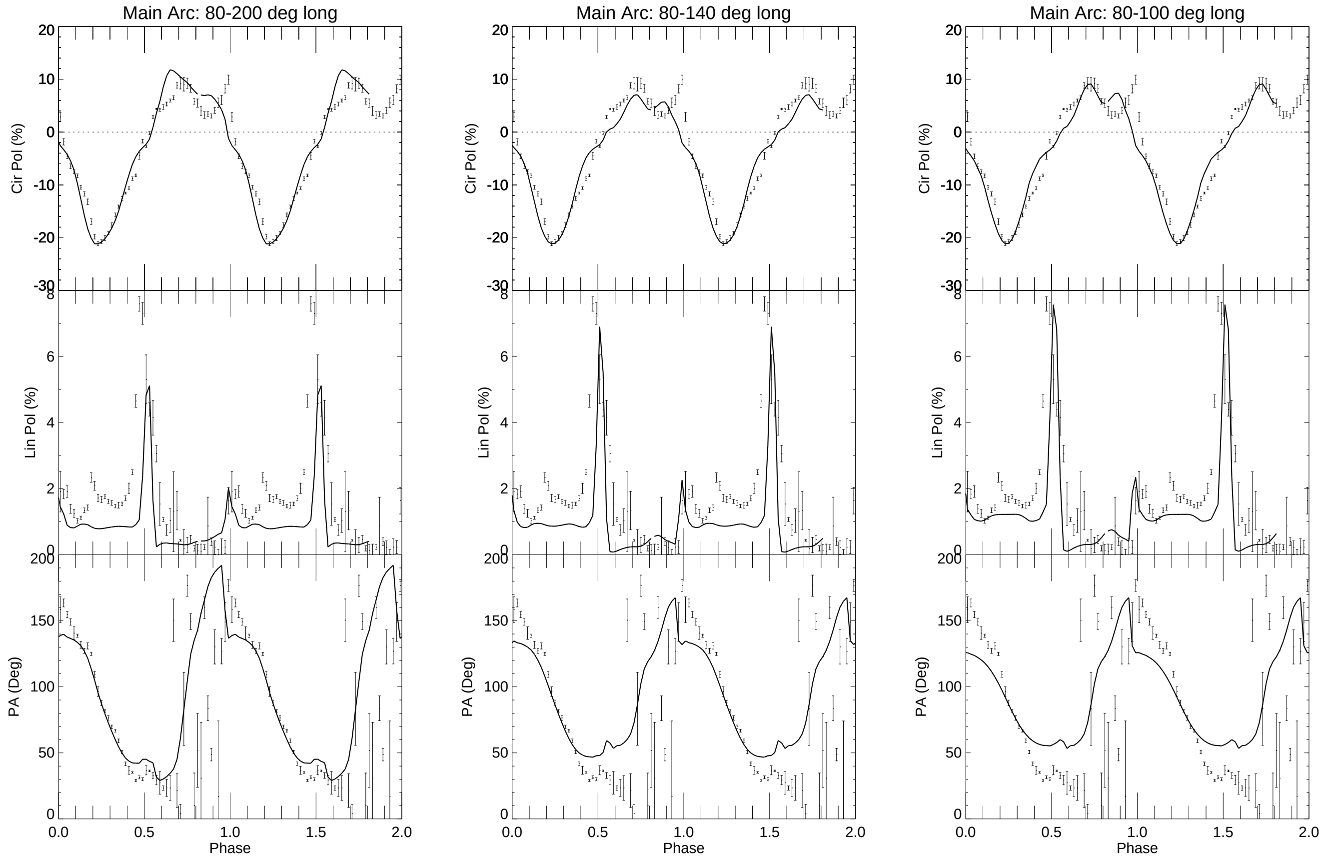

Figure 5. The model fits overlayed upon the red filter data for a main accretion arc of 3 different lengths: from left to right a range in mag long of 80–200° (as before), 80–140° and 80–100°. The other parameters and length of the secondary accretion region remain unchanged from table 3.

Piirola, V., Coyne, G. V., Takalo, L., Larsson, S. & Vilhu, O., 1994, A&A, 283, 163

Ramsay, G., Rosen, S. R., Mason, K. O., Cropper, M. & Watson, M. G., 1993, MNRAS, 262, 993

Ramsay, G., Mason, K. O., Cropper, M., Watson, M. G. & Clayton, K. L., 1994, MNRAS, 270, 692

Silber, A. D., Remillard, R. A., Horne, K. & Bradt, H. V., 1994, ApJ, 424, 955

Stockman, H. S., Schmidt, G. D., Liebert, J. & Holberg, J. B., 1994, ApJ, 430, 323

Unger, S. W., Taylor, K., Pedlar, A., Ghataure, H. S., Penston, M. V., Robinson, A., 1990, MNRAS, 242, 33P

Wickramasinghe, D. T. & Meggitt, S. M. A., 1985, MNRAS, 214, 605

Wu, K. & Wickramasinghe, D. T., 1993, MNRAS, 260,141

Wu, K., Wickramasinghe, D. T., Bailey, J. & Tennant, A. F., 1994, PASA, 11, 198

Zimmermann, H. U., Becker, W., Belloni, T., Döbereiner, S., Izzo, C., Kahabka, P & Schwentker, O., 1994, MPE report 257